MICROFRACTRUE MECHANISM OF TA2/A3 EXPLOSIVE CLADDING INTERFACE①

Yang, Yang Zhang, Xinming
Department of Materials Science and Engineering, Central-South University of Technology, Changsha 410083
Li, Zhenghua Li, Qingyun
North-West Institute for Nonferrous Metal Research

ABSTRACT: In-situ SEM observations on the TA2/A3 explosive cladding interfaces had been performed to examine their microfracture behaviour. The important conclusions of the study were summarized as follows. The microfracture mechanism of explosive cladding TA2/A3 interface are: (1) microcracks initiate inside the swirls or inside the molten material as well as on the boundary between the molten material and the A3 matrix, which penetrate into the nearby A3 matrix in the direction normal to the tensile loading direction under the action of the crack-tip stress field, (2) at the same time of the action of mechanism(1), microcracks initiate along the TA2/A3 interface, and link up under the tensile load. Terminal cleavage fracture takes place mainly in the recrystallized and grain abnormal growth region on the A3 side in the vicinity of TA2/A3 interface. No crack nucleation and propagation inside the adiabatic shear band (ASB) on the TA2 side were observed under the tensile load at room temperature. It is necessary to avoid the jetting molten material wrapped up in the swirl by controlling the collision parameters.

Key words: microfracture mechanism explosive cladding interface

1 INTRODUCTION

The explosive cladding technique makes it possible to clad pairs of metals or alloys having widely different properties, which can extend the properties and usages of metals as well as alloys. The "metallurgical bond" of the explosive cladding is obtained by the action of localized melting and diffusion processes at the contacted surface[1]. The properties of metals (e.g. strength, melting point, etc) and collision parameters (e.g. explosivers, e/m ratio, and the stand-off distance, etc) will affect the pressure and its distribution, jet thickness and the bonding interface morphology. Usually three kinds of interface morphologies were obtained: (1) small wavy interface, (2) medium wavy interface and (3) large wavy interface with moten material in swirl.

Recent attempts have been made to study the fatigure failure mechanisms of the explosive cladding interface[2, 3]. However, no work on the microfracture mechanism of explosive cladding interface under tensile load have been reported. In the present study a miniature tensile specimen was used in the SEM so that the sequence of failure by crack initation and growth could be observed and recorded in-situ as the tensile load increased incrementally. However, because of the relaxation of internal stresses at the surface, there are quantitative difference between sample and bulk behavior. The surface effects on the fracture behavior have been examined analytically by Humphreys[4].

2 EXPERIMENTAL PROECDURES

The materials used in this study were commercial pure titanium (TA2) and mild

① Received Sept 14, 1994; accepted in the revised form Oct. 10,1994

steel (A3). Three kinds of interface morphorogy were obtained by using different collision parameters. Specimens were cut from the central portion of the sheets in a plane parallel to the direction of jetting and normal to the plane of the clad interface by spark erossion. The TA2 side of the TA2/A3 composite plate was linked with the same state TA2 plate by argon-arc weld. The central line of the heat affected zone of argon-arc weld was 6 mm away from the explosive cladding interface and had no effects on the TA2/A3 interface. Then, the specimens were mechanically and chemically polished successively.

Fig. 1 shows the scheme of the fracture. Its thickness is 0.25mm. Investigations of the microfracture mechanisms in tension specimens were performed with an electronically controlled loading device mounted in KYKY-AMRAY 1000B scanning electron microscope. The fractographic analysis was performed with X-650 scanning electron microscopy equiped with EDS.

3 RESULTS

The microstructure of the three kinds of TA2/A3 interface are shown in Fig. 2. EDS analysis of the molten region in swirl of Fig. 2 (c) indicated that the molten material had a composition of 49 at.-% Ti and 51 at.-% Fe. The room temperature tensile properties of these composites are listed in Table 1.

Table 1 Tensile properties of TA2/A3 composite

properties	TA2	A3	TA2/A3 composite*		
			small wavy	medium wavy	large wavy
strength σ_b/MPa	452	476	495	487	480
elongation σ_b%	42	30	28.5	27	25.5

* tensile experiment performed according to the requirements of GB8547-87

Fig. 3 illustrates the crack initiates and fracture spreads progressively in the small wavy interface under tension stress. At 150MPa, microcracks occur along the TA2/A3 interface(Fig. 3(a)). With load further increased the microcracks coalesce(Fig. 3(b-d)) along the interface, and at the same time some other microcracks occur in the TA2 and A3 matrix(Fig. 3(c-d)). Prior to the final fracture, two steps of failure were observed i.e.

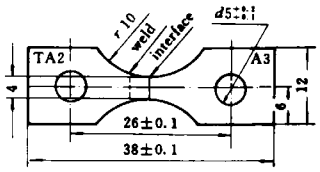

Fig. 1 Schematic representation of fracture test specimen

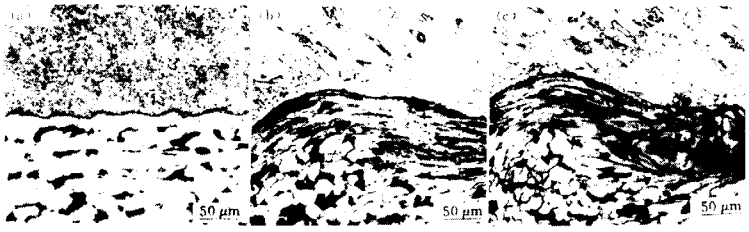

Fig. 2 Microstructrue of the three kinds of cladding interface morphorogies
(a)—small wavy; (b)—medium wavy; (c)—large wavy

(1)cavities appear along the TA2/A3 interface (Fig. 3(a))

(2)coalesce occurs along the TA2/A3 interface and microcracks occur in TA2 and A3 matrix (Fig. 3(c-d)).

Fig. 4 shows the microfracture sequence of interface with medium wave. At the load of 330 MPa, microcrack occurs in the swirl zone (Fig. 4(a)). As the load increased from 330 MPa to 400 MPa, the crack opening displacement also increased from 0. 3 μm to 3. 4 μm (Fig. 4(a-c)), and the microcracks were observed to be linked up along the flow line and resulted in crack propagation (Fig. 4(b-c)). Intensive three-dimensional stress exists near the crack-tip, so that the crystal defects are sensitive to this region. The crack-tip is blunted by absorbing[5-6] and emitting[7] dislocations. After the main crack becomes blunt, the crack grows steadily in the way of a microcrack formed in a distance from the front of the maincrack by stress concentration, and the main crack linked up with the front microcrack by necking of the crack bridge (Fig. 4(a-c)). The steady propagation direction of crack was normal to the tensile load direction.

At the same time, the microcracks occur, link up and propagate along the TA2/A3 interface with the increasing of tensile load (Fig. 4(d-e)), which results in unsteadily rapid fracture along the TA2/A3 interface (Fig. 4(f)).

Initially, at a stress of 350 MPa, cracks predominantly occur on the boundary between the molten region and the A3 matrix (Fig. 5(a)) as well as in the molten region. As the load increases, the number of cracks in the molten region increases (Fig. 5(b-c)) and the crack opening displacement on the boundary between the molten region and the A3 matrix increases to ~10μm (Fig. 5(c)), crack propagates into the A3 matrix under the action of the crack-tip stress field. After the crack blunting, crack grows steadily in the way of a

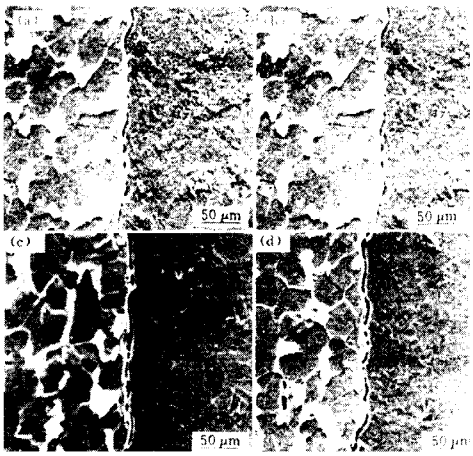

Fig. 3 Processes of cracking of small wavy interface at incremental values of tension load
(a)—150 MPa; (b)—178 MPa; (c)—350 MPa; (d)—476 MPa

microcrack formed at the crack tip due to stress concentration(Fig. 5(a-c)). The steady propagation direction of crack is normal to the loading direction, which reveals the effects of the principal stress on the crack propagation.

In the process of crack initiation, propagation and final fracture of the specimen, no microcracks were observed in adiabatic shear bands (ASB,) (Fig. 4). It illustrates that ASB, is not the place where the microcracks

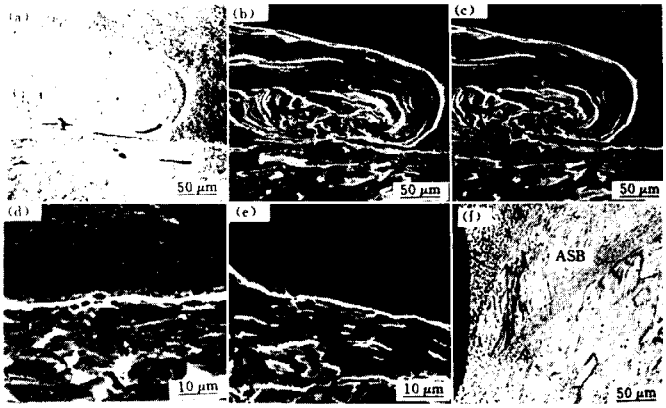

Fig. 4 The SEM-graph of the crack propagation along the flow line in swirl of medium wavy interface at incremented values of load and cracks inition/propagation along the medium wavy interface at incremented values of loads appearance on the TA2 side after fracture
(a)—330 MPa, (b)—380 MPa, (c)—400 MPa; (d)—200 MPa, (e)—330 MPa; (f)—OM

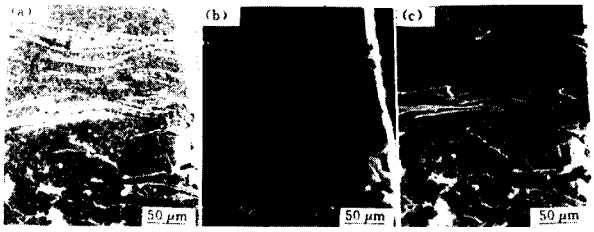

Fig. 5 A SEM-graph of the propagation of cracks in the molten region at incrementecl values of load
(a)—350 MPa; (b)—380 MPa; (c)—400 MPa

easily nucleated and propagated under tensile load at room temperature.

The fractography shows that the fracture surface shows predominatingly cleavage feature (Fig. 6). EDS analysis show that there are all Fe and no Ti exists on the cleavage fracture surface on both sides of TA2 and A3 indicating that the cleavage fracture takes place on the A3 side in the vicinity of the TA2/A3 interface. The fractograph of the molten region in swirl is shown in Fig. 7, EDS analysis shows that there are Fe and Ti existed in this region. Localized fracture has taken place in the molten layer (Fig. 8) of interface.

The grain in the molten layer (Fig. 8(b-c)) is very small, and EDS analysis shows that the composition is about 49(at.-%) Ti and 51(at.-%) Fe.

From the above facts, the general process of microfracture in the TA2/A3 explosive cladding interface under tensile load can be summarized as follows:

(1) microcracks initiate inside the swirls (Fig. 4(a)) or inside the molten regions as well as on the boundary between the molten region and A3 matrix (Fig. 5(a)), and penetrate into the nearby A3 matrix along the direction normal to the tensile load under the action of the crack-tip stress field.

(2) at the same time of the action of mechanism(1) microcracks initiate along the TA2/A3 interface and link up under the tensile load (Fig. 4(d-e)). The final cleavage fracture takes place mainly on the A3 side in the vicinity of TA2/A3 interface (Fig. 6-7). Localized fracture takes place along the

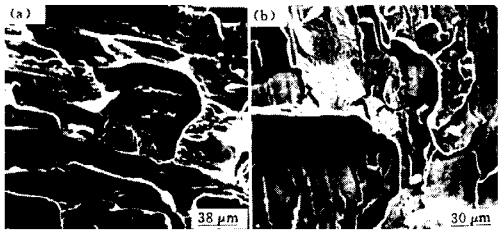

Fig. 6 SEM-graph of the fractured surface
(a)—on the A3 side; (b)—on the TA2 side

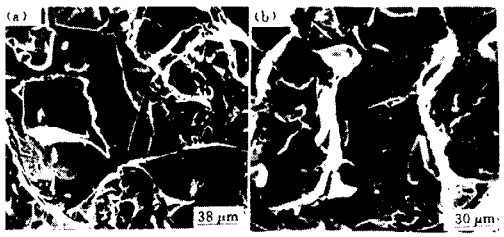

Fig. 7 SEM-graph of the fractured surface of the molten material in swirl
(a)—on the A3 side; (b)—on the TA2 side

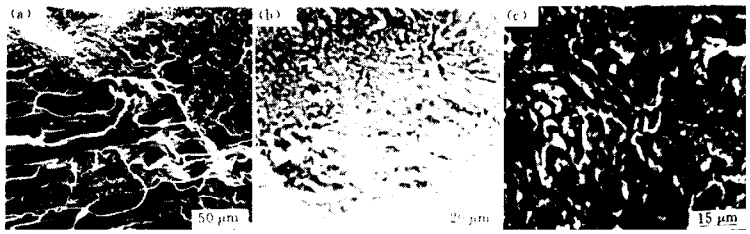

Fig. 8 SEM-graph of the fractured surface of molten layer
(a)—the fractured surface on the TA2 side (include cleavage fractured surface and fractured surface from interface molten layer);
(b)—the detail of the upper parts in (a);
(c)—the fractured surface of molten layer on A3 side

molten layer of interface (Fig. 8).

(3) No crack nucleation and propagation inside the ASB on the TA2 side of TA2/A3 interface were observed under tensile load at room temperature (Fig. 4(f)).

4 DISCUSSION

Stroh[8] proposed that the stress concentration forms at the tip of slip band where dislocations are piled up, which causes a crack nucleus. The critical stress at which the cleavage crack nucleus propagation is given by Cottrell[8] as follow:

$$\sigma_c \geqslant 2\mu r/(K_y^* \sqrt{d}) \qquad (1)$$

where μ is the shear modulus, r is the surface energy, d is the grain diameter, and K_y^* is a material constant.

It can be seen from the equation (1) that the critical stress for the crack propagation increases linearly with $d^{-1/2}$, thus the growth of grains tends to make the metal brittle.

Our prior works on the microstructure of bonded zone in an explosive cladding TA2/A3 system[11] have shown that the residual structure around the TA2/A3 explosive cladding interface are the interface layer, the heat affected zone (recrystallized and recorved region) as well as deformation zone on the A3 side, and the ASB, on the TA2 side.

The residual recrystallized and grain abnormal growth structure near the interface layer on the A3 side is the place where the cleavage fracture easily takes place.

The residual stress is tensile on A3 side and compression on TA2 side[10]. The residual tensile stress can accelerate the crack's nucleation and propagation.

The characteristics of the structure residual stress distribution around the TA2/A3 explosive cladding interface and the factograph as well as composition analyse on the fractured surface are considered to be the reasons why the cleavage fracture mainly takes place on the A3 side in the vicinity of the cladding interface.

5 CONCLUSION

(a) The microfracture mechanisms of the explosive cladding interface are;

(1) microcracks initiate inside the swirls or the molten region as well as on the boundary between the molten region and the A3 matrix. They penetrate into the nearby matrix along the direction normal to the loading direction.

(2) at the same time of action of mecha-

nism (1), microcracks initiate along the TA2/A3 interface and link up under tensile load. The final cleavage fracture of the specimen takes places mainly in the recrystallized and grain abnormal growth regions on the A3 side in the vicinity of TA2/A3 interface. Localized fracture takes place along the interface molten layer.

(b) No cracks nucleation and propagation inside the adiabatic structure and ASB, on the TA2 side of TA2/A3 interface are observed under tensile load at room temeprature.

REFERENCE

1 Yang, Y; Zhang, X M; Li, Z H; Li, Q Y. Trans of Nonferrous Metals Soc of China 1994, 4(3): 98.
2 Duan, W S; Lu, H M; Lin, J X; Wu, J Z. Rare Metal Materials and Engineering, 1989, (3): 22.
3 Lu, H M; Duang, W S. Rare Metal Materials and Engineering, 1989, (2): 19.
4 Humphreys, F J. In: Proc of the EMAG-MICRO 89, Lonton: September, 1989, 465.
5 Yoshii, K; Kawobe, H; Yamada, T. Mechanical Behavior of Materials, 1972, (1): 256.
6 Forsth, P J; Wilson, R N. J Inst Met, 1963, 92, 82.
7 Tetelman, A S; Robertson, W D. Acta met, 1963, (11): 415.
8 Stroh, A N. In: Proc Roy Soc R54, 223A, 404. 1955, 232A, 548.
9 Cottrell, A H. Trans, AIME, 1958, 212, 192.
10 Weiss, B Z. Z Metallkde, 1971, 62, 159.

(*From page 112*)
formed α_2/γ grains. Thus fine duplex microstructure composed of α_2/γ lamellar strucutre and equiaxed γ phase grain with same volume fraction was obtained (Fig. 3 Ⅲ (c)).

5 CONCLUSIONS

(1) Two-step heat treatment can decrease or eliminate large untransformed lamellar structure. Suitable first heaing temperature and cooling rate can gain homogeneous, fine duplex microstructure with the same volume fraction of equiaxed γ grains and α_2/γ lamellar structure.

(2) TiAl alloy room-temperature tensile properties can be remarkably improved by two-step heat treatment, and room-temperature ductility reached 3.3%.

REFERENCES

1 Kim, Y W. JOM, 1989, 41(7): 21—29.
2 Lipsitt, H A. In: Proc of Nicholas J Grant Symp, 1985.
3 Bondarev, B; Anoshkin, N *et al.* In: Proc of International Symp On Intermetallic Compounds—Structure and Mechanical Properties, June, 1991.
4 Kong, Gaoning. MS Thesis, Central South University of Technology, 1994.
5 小林郁夫, 吉原美知子, 田中良平. 日本金属学会志, 1989, 53(2): 251—252。